Clin. Lab. 2026;72:XXX-XXX

ORIGINAL ARTICLE

Prediction Model for Monoclonal Gammopathy of Renal Significance Risk in Nonmalignant Monoclonal Disorders

Jianrong Yang, Qiongxu Li, Furong Ying, Mengjia Chen, Meijuan Zhang

Department of Laboratory Medicine, The First Affiliated Hospital of Wenzhou Medical University, Wenzhou, China

SUMMARY

Background: **The aim is to identify independent risk factors for monoclonal gammopathy of renal significance (MGRS) and develop a predictive model for optimizing renal biopsy decision-making in suspected patients, thereby improving biopsy positivity rates.**

Methods: **We retrospectively enrolled 291 patients from The First Affiliated Hospital of Wenzhou Medical University (January 2015 - December 2022). Clinical and laboratory indicators were collected. Independent predictors of MGRS were screened using Least Absolute Shrinkage and Selection Operator (LASSO) regression and multivariate logistic regression, followed by the construction of a nomogram model. Patients were randomly divided into training (n = 204, 70%) and validation (n = 87, 30%) cohorts. Model performance was evaluated in the independent validation set via ROC analysis, calibration curves, decision curve analysis (DCA), and Hosmer-Lemeshow (HL) test.**

Results: **Among 291 patients, 132 (45.4%) were MGRS-positive. Five independent predictors were identified: abnormal free light chain (FLC) ratio, advanced age, abnormal white blood cell count, hypoglobulinemia, and 24-hour urinary protein > 1.5 g. The model exhibited excellent discrimination, with an AUC of 0.823 (95% CI: 0.767 - 0.879) in the training set and 0.912 (95% CI: 0.854 - 0.971) in the validation set. Calibration parameters approximated ideal values in both sets (training: intercept = -0.00, slope = 1.00; validation: intercept = -0.05, slope = 1.07). HL test confirmed optimal goodness-of-fit (training: $\chi^2 = 7.395$, p = 0.495; validation: $\chi^2 = 3.631$, p = 0.889). DCA demonstrated significant net clinical benefit across threshold probabilities.**

Conclusions: **This validated MGRS predictive model (AUC > 0.9 in independent validation) shows high accuracy and clinical utility for noninvasive screening of high-risk patients and individualized renal biopsy decisions.**

(Clin. Lab. 2026;72:xx-xx. DOI: 10.7754/Clin.Lab.2025.250714)

Correspondence:
Meijuan Zhang
Department of Clinical Laboratory
Key Laboratory of Clinical Laboratory Diagnosis and Translational Research of Zhejiang Province
The First Affiliated Hospital of Wenzhou Medical University
Wenzhou
Zhejiang
China
Email address: 18767482298@126.com

Manuscript accepted September 11, 2025

KEYWORDS

MGRS, monoclonal immunoglobulin, renal injury, predictive factors, nomogram

INTRODUCTION

MGRS is a condition primarily characterized by renal damage caused by monoclonal immunoglobulin deposition. Due to its insidious onset and high misdiagnosis rate, MGRS differs significantly from non-monoclonal immunoglobulin-related chronic kidney disease (CKD) in terms of treatment and prognosis. Klomjit N et al. demonstrated [1] that only 160 out of 6,300 patients with monoclonal gammopathy (MG) underwent renal biop-

sy, accounting for just 2.5% of the cohort. Among these 160 patients, 64 (40%) exhibited MGRS-related lesions, underscoring the critical role of renal biopsy in diagnosing MGRS. However, the low rate of renal biopsy performance often results in delayed detection and treatment of MGRS, making early diagnosis increasingly vital in clinical practice [2-4].

Currently, MGRS is defined by the presence of renal impairment, evidence of monoclonal protein deposition in renal biopsy, and adherence to the diagnostic criteria for monoclonal gammopathy of undetermined significance (MGUS) [5]. Although renal biopsy remains the gold standard for diagnosis, its widespread application is limited by low patient compliance with invasive procedures and the technical challenges associated with renal puncture. Therefore, there is an urgent need to develop a simple, cost-effective, and non-invasive diagnostic approach, which holds significant clinical value for the early detection and management of MGRS.

This study adopts a retrospective design to analyze data from patients in the Department of Nephrology at the First Affiliated Hospital of Wenzhou Medical University. The aim is to identify independent risk factors associated with MGRS and to construct a predictive model using machine learning techniques. This model aims to assist clinicians in evaluating patients suspected of having MGRS, thereby guiding selective renal biopsy decisions. By minimizing unnecessary biopsies while promoting renal puncture in patients with a high likelihood of MGRS, this approach seeks to improve the early diagnosis rate of MGRS, optimize treatment pathways, and reduce the risk of progression to end-stage renal disease or hematological malignancies.

MATERIALS AND METHODS

Research object and methodology

Research object

The study included a total of 291 patients who visited the First Affiliated Hospital of Wenzhou Medical University between January 2015 and December 2022. The study protocol was approved by the Ethics Committee in Clinical Research (ECCR) of the First Affiliated Hospital of Wenzhou Medical University (approval number: KY2024-R087). Given the retrospective nature of the study and the use of anonymized data, the requirement for informed consent was waived.

Diagnostic criteria for MGRS: The criteria include [6]: 1) Evidence of kidney damage associated with monoclonal immunoglobulin (MiG) produced by the monoclonal proliferation of B cells, monoclonal B lymphocytes, or plasma cells; 2) Absence of tumor complications or failure to meet the current diagnostic criteria for hematological malignancies requiring specific treatment; 3) Pathological types of MGRS encompass immunoglobulin-related amyloidosis, fibrous glomerulonephritis, immune complex-mediated glomerulopathy, type I cold agglutinin glomerulonephritis, light chain-related tubular lesions, crystal-storing histiocytosis, monoclonal immunoglobulin deposition disease, monoclonal IgG deposition proliferative glomerulonephritis, and C3 nephropathy associated with monoclonal immunoglobulins.

Inclusion criteria: 1) Patients who underwent renal biopsy and provided complete clinical and pathological data; 2) Upon admission, patients exhibited abnormalities in one or more of the following tests: serum protein electrophoresis (SPEP), blood immunofixation electrophoresis (IFE), urine immunofixation electrophoresis (IFE), and blood and urine FLC testing; 3) Patients had not received treatments such as chemotherapy or autologous stem cell transplantation prior to admission.

Exclusion criteria: 1) Patients diagnosed with multiple myeloma, smoldering myeloma, Waldenström's macroglobulinemia, chronic lymphocytic leukemia, malignant lymphoma, or other lymphoid plasma cell neoplasms; 2) Patients who did not undergo renal biopsy; 3) Patients with incomplete clinical data.

Research methods

Data collection method

The data utilized for this research were obtained from the medical records of patients during their hospitalization at the First Affiliated Hospital of Wenzhou Medical University. This data encompasses a range of documents, including but not limited to admission records, discharge summaries, clinical course notes, medical orders, laboratory test results, and nursing documentation.

Collection of basic information

This study collected baseline information from patients who exhibited monoclonal immunoglobulins in their blood and underwent renal biopsy. The data included variables such as age, gender, clinical manifestations at disease onset, presence of hypertension, and duration of kidney disease. Based on renal pathological findings, patients were categorized into two groups: the MGRS-negative group and the MGRS-positive group. The distribution characteristics of these two groups were then analyzed using descriptive and statistical methods.

Indicators for laboratory testing

This study meticulously compiled the results of laboratory tests conducted upon patients' admission to the hospital. The comprehensive set of recorded indicators included routine biochemical parameters, such as alanine aminotransferase, creatinine, and albumin, as well as hematological parameters, encompassing white blood cell and red blood cell counts. The analysis also incorporated metrics of blood clearance and urine FLC levels, which comprised both concentration and the serum free light chain k/λ ratio. Furthermore, serum and urine immunofixation electrophoresis, along with other relevant indicators, were integrated into the study's analysis.

Renal histopathological biopsy

A renal puncture biopsy was conducted utilizing ultrasound guidance, and the kidney tissue samples obtained were analyzed through optical microscopy, immunopathology, and electron microscopy. The results of the biopsy were collaboratively assessed by experts from the Department of Pathology and Nephrology at the First Affiliated Hospital of Wenzhou Medical University to ascertain the presence of monoclonal deposition within the kidney tissue.

Rationale for variable selection in the MGRS prediction model

Based on clinical relevance and evidence derived from nephrology/hematology guidelines, this study ultimately selected 11 predictors for inclusion in the model. Abnormal FLC ratio is a hallmark diagnostic indicator, with sensitivity up to 93.8% and specificity approximately 82%. It reflects the production and deposition of monoclonal light chains directly damaging the kidneys. Monoclonal immunoglobulin type (light chain only) is present in approximately 90% of MGRS cases, where κ/λ light chain deposition triggers renal lesions.

Bone marrow plasma cell percentage (≥ 10%) serves as the diagnostic cutoff for distinguishing MGRS from MGUS and correlates with the severity of renal lesions [6,7]. Age over 60 years has been demonstrated to be significantly associated with increased risk, primarily attributed to immunosenescence and decreased renal functional reserve [8,9]. Elevated white blood cell count ($> 10 \times 10^9$/L) may indicate underlying inflammation or immune dysregulation, potentially contributing to renal injury [7,10]. Anemia (Hb < 120 g/L in males, < 110 g/L in females) is associated with disease progression and renal impairment, serving as a surrogate marker for systemic toxicity [6,9]. Reduced estimated glomerular filtration rate (eGFR < 60 mL/minute/1.73 m^2) directly correlates with the degree of renal injury [8,10]. Increased 24-hour urine protein excretion (> 1.5 g) suggests glomerular or tubular damage and is associated with adverse renal outcomes [7,9]. Serum albumin level reflects nutritional status, chronic inflammation, or liver dysfunction in MGRS patients. Abnormal total protein (elevated or decreased) indicates dysregulated protein metabolism associated with monoclonal gammopathy.

Sample size calculation

The sample size calculation for this study was performed using the method proposed by Riley et al. [11], which is based on the expected model explained variance (R^2). This approach comprehensively considered the number of predictors (k = 11), the outcome event incidence rate (p = 2.5%), and model validation requirements to determine the minimum necessary sample size. In accordance with common recommendations for developing clinical prediction models in low-event-rate contexts [12,13], we adhered to the "at least 10 events per variable" (EPV) rule as a foundational guideline. Based on the average explained variance (Avg (R^2) = 0.1) observed in similar studies and adhering to the "at least 10 events per variable" (EPV) rule, an initial baseline sample size was estimated. Fifteen percent (15%) of data points exhibiting missing values were handled using Multiple Imputation by Chained Equations (MICE). The total sample was then randomly divided into a training set (n = 204, 70%) and an independent validation set (n = 87, 30%) in a 7:3 ratio. The model was developed on the training set and its performance was subsequently evaluated on the validation set.

The final target sample size of 289 cases ensures at least 25 positive outcome events in the disease group. This not only exceeds the minimal EPV requirement but also satisfies the more stringent 5 × EPV threshold criterion (requiring 55 events for k = 11 predictors), which is advocated for enhanced model stability and reliability in validation. This sample size demonstrates robust model performance metrics (AUC, sensitivity/specificity), with a 95% confidence interval width ≤ 0.1. This satisfies the requirement for stability in clinical prediction models.

Statistical methods

The statistical analyses were performed using R software (version 4.2.1; R Foundation for Statistical Computing, Vienna, Austria). All continuous variables were first assessed for normality using the Shapiro-Wilk test. For data conforming to a normal distribution, independent samples *t*-tests were applied after confirming homogeneity of variance with Levene's test, while non-normally distributed data were analyzed using the Mann-Whitney U test, with corresponding effect sizes reported (Cohen's d for parametric tests and rank-biserial correlation coefficient for non-parametric tests). Categorical variables were analyzed using either Pearson's χ^2 test with Yates' continuity correction or Fisher's exact test, selected based on expected frequencies. Variable selection followed a multi-stage strategy: initial screening through univariate analysis (Spearman's rank correlation for continuous variables and χ^2/Fisher's exact test for categorical variables, retaining those with p < 0.1), followed by dimension reduction via LASSO regression with 10-fold cross-validation using stratified sampling to maintain outcome proportions, where the optimal λ value was selected using the 1-SE rule. The final model was constructed through multivariable logistic regression including variables meeting the entry criterion (p < 0.05) while excluding those showing multicollinearity (VIF ≥ 5). Model performance was evaluated on an independent validation set, assessing discrimination (AUC with 95% CI and optimal cutoff determined by Youden index), calibration (calibration curve and HL test), and clinical utility (DCA). Internal validation used 1,000 bootstrap samples with replacement, drawn from the original cohort. For each sample, we recalculated model coefficients and performance metrics. The final reported CIs represent the 2.5th - 97.5th percentiles of bootstrap distributions. The specific workflow is shown in Figure 1.

Table 1. Comparison of clinical data and laboratory indicators.

Variable	All-Patients (n = 291)	Non-MGRS (n = 159)	MGRS (n = 132)	p-value
Age	59.32 (50.96, 67.86)	57.79 (50.19, 66.05)	62.87 (53.06, 69.75)	0.011
Fcm	0.36 (0.34, 0.41)	0.36 (0.36, 0.36)	0.36 (0.33, 0.48)	0.875
LC Type				
0	266 (91)	144 (91)	122 (92)	0.724
1	25 (9)	15 (9)	10 (8)	
WBC (10^9/L)	6.5 (5.48, 7.44)	6.23 (4.95, 7.16)	6.68 (5.73, 7.89)	0.001
RBC (10^{12}/L)	4.1 (3.64, 4.43)	4.04 (3.46, 4.49)	4.13 (3.83, 4.41)	0.102
Hb (g/L)	124 (111.24, 135.62)	121 (106.94, 135.35)	124.56 (119.21, 135.86)	0.021
TP (g/L)	58.41 (50.68, 64.22)	61.68 (52.2, 68.24)	55.36 (49.4, 60.29)	< 0.001
Alb (g/L)	27.35 (22.56, 32.3)	29.9 (22.79, 34.65)	26.3 (21.85, 30.76)	< 0.001
24 hours UTP > 1.5 g				
0	62 (21)	57 (36)	5 (4)	< 0.001
1	229 (79)	102 (64)	127 (96)	
eGFR (mL/minute)	75.25 (43.27, 91.5)	60.09 (34.46, 88.86)	79.29 (64.53, 92.3)	< 0.001
FLC Rtn Abn				
0	216 (74)	141 (89)	75 (57)	< 0.001
1	75 (26)	18 (11)	57 (43)	
Globulin (g/L)	29.4 (25.17, 32.57)	29.88 (6.07, 33.54)	27.79 (4.66, 31.85)	0.010
A/G	0.96 ± 0.26	0.97 ± 0.28	0.94 ± 0.23	0.367

Fcm Proportion of flow cytometry plasma cells, LC Type the type of light chain, 0 Not light chain, 1 light chain, WBC white blood cell, RBC red blood cell, Hb hemoglobin, TP total protein, Alb Albumin, 24 hours UTP > 1.5 g total urinary protein exceeding 1.5 g/24 hours, eGFR estimated glomerular filtration rate, FLC Rtn Abn the abnormal free light chain (FlC) ratio, A/G the ratio of albumin to globulin.

Table 2. Single-factor and multi-factor logistic regression analysis.

Variable	Univariate OR (95% CI)	Uni-p	Multivariate OR (95% CI)	Multi-p
Globulin (g/L)	0.945 (0.899 - 0.988)	0.019	0.909 (0.852 - 0.959)	0.001
FLC Rtn Abn	7.305 (3.515 - 16.48)	< 0.001	8.310 (3.498 - 22.04)	< 0.001
eGFR (mL/minute)	1.01 (1.001 - 1.02)	0.024		
24 hours UTP > 1.5 g	10.12	< 0.001	9.577	< 0.001
Alb (g/L)	0.946 (0.905 - 0.988)	0.014		
TP (g/L)	0.955 (0.927 - 0.982)	0.002		
WBC (10^9/L)	1.335 (1.135 - 1.595)	< 0.001	1.411 (1.153 - 1.768)	0.002
Age	1.026	0.043	1.065	< 0.001

WBC white blood cell, TP total protein, Alb Albumin, 24 hours UTP > 1.5 g total urinary protein exceeding 1.5 g/24 hours, eGFR estimated glomerular filtration rate, FLC Rtn Abn the abnormal free light chain (FlC) ratio.

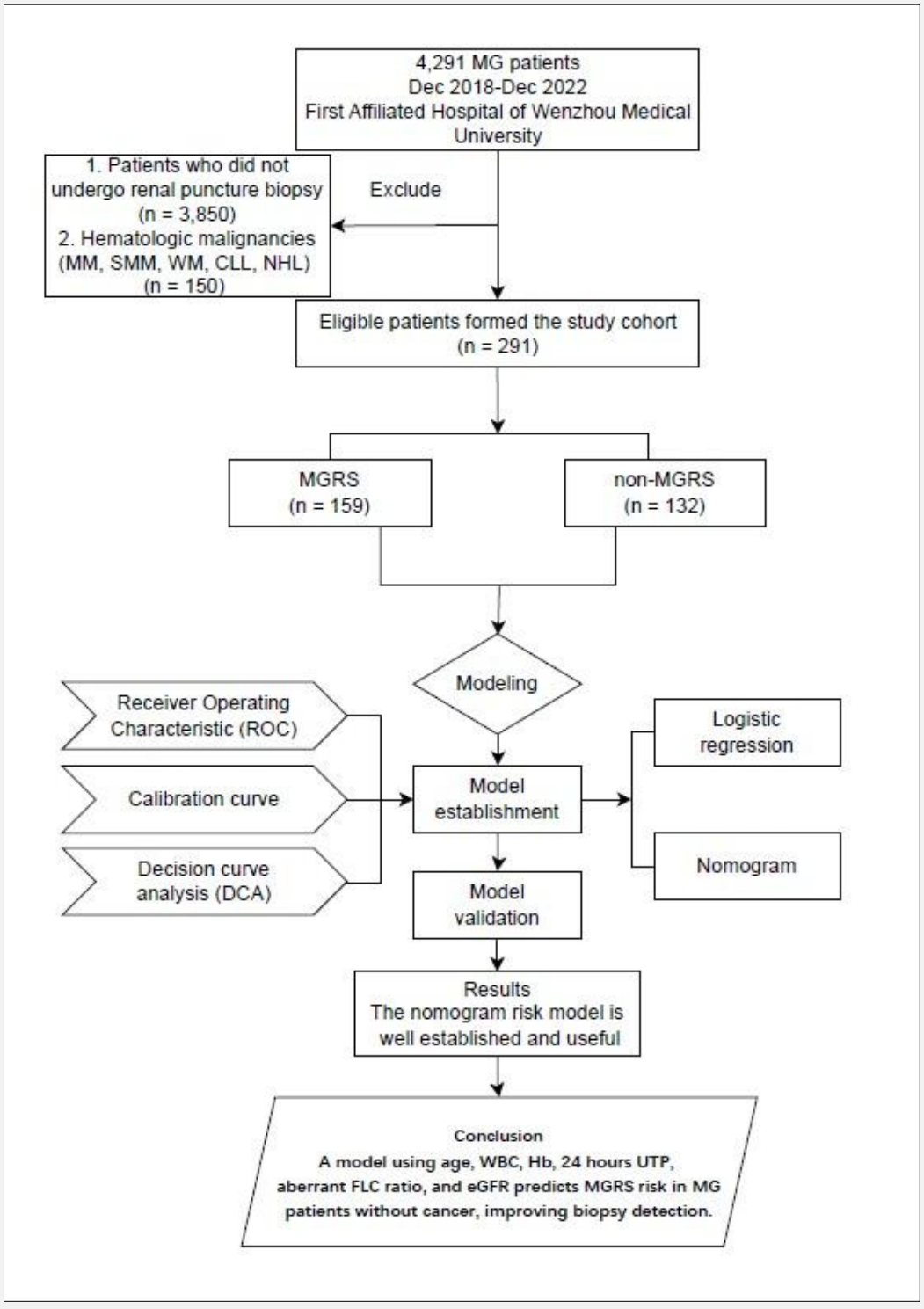

Figure 1. Flowchart of patient selection and MGRS risk model development.

The diagram illustrates the screening process of 15,709 MG patients at the First Affiliated Hospital of Wenzhou Medical University (December 2015 - December 2022). After excluding 15,222 patients without renal biopsy and 196 with hematologic malignancies, 291 eligible patients were stratified into MGRS (n = 159) and non-MGRS (n = 132) groups. The model was developed using logistic regression (incorporating age, WBC, Hb, 24-hour urine protein, aberrant FLC ratio, and eGFR) and validated via ROC analysis, calibration curves, and DCA. The final nomogram effectively stratifies MGRS risk in MG patients without hematologic malignancies.

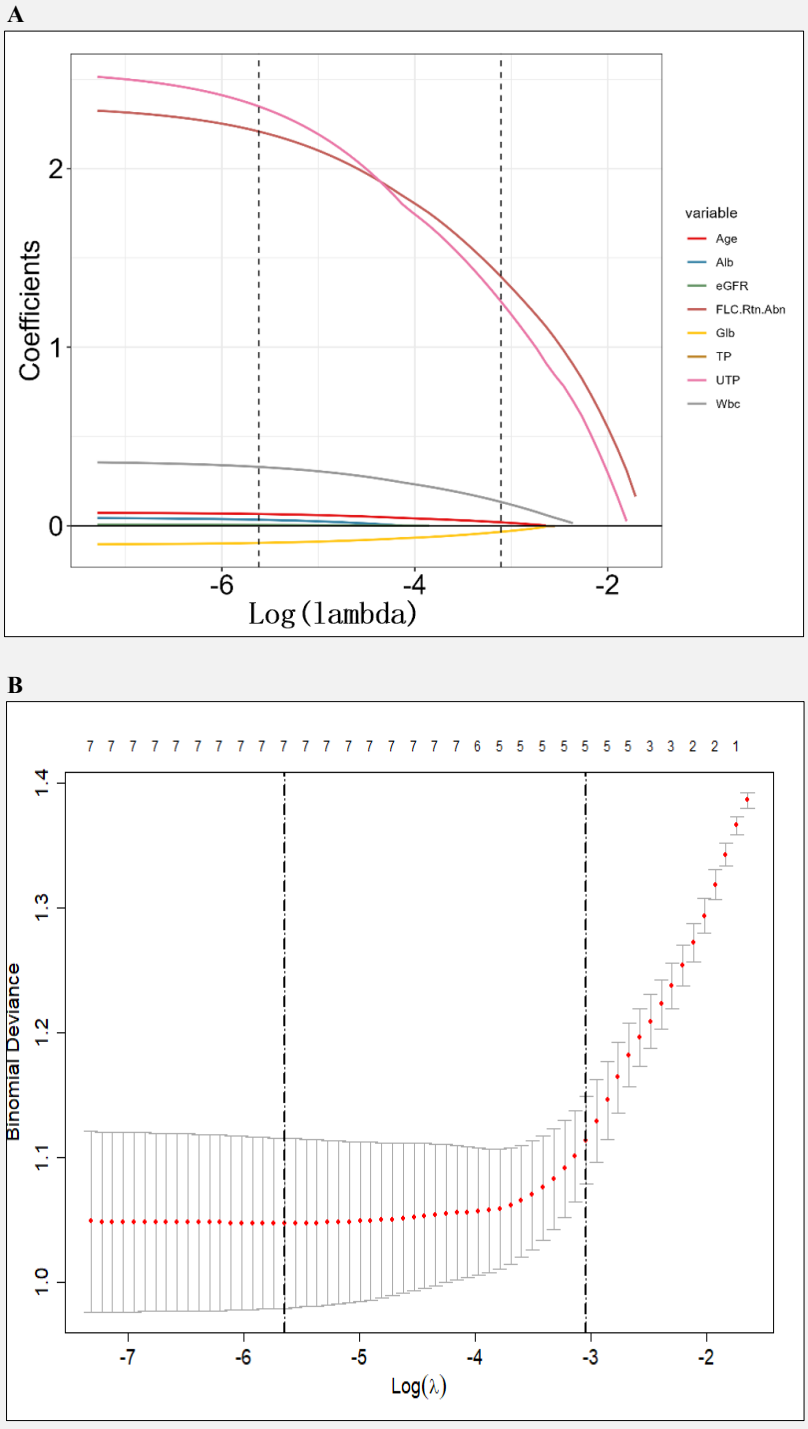

Figure 2. Coefficient trajectories and model deviance in MGRS risk prediction

A Coefficient trajectories showing variable selection across log λ values (-7 to -2). Colored curves represent different predictors, with shrinkage effects observed as λ increases. In our LASSO regression analysis, we utilized the lambda 1 se value (lambda = 0.04478383) as our final tuning parameter, which corresponds to log (lambda) = -3.11. B The plot shows the binomial deviance (mean ± 1 standard error) across a range of log (λ) values. The red dashed line indicates the position of the optimal λ (λ.1 se = 0.045, log (λ.1 se) = -3.11), which was selected using the 'one standard error rule' to yield the most parsimonious model within one standard error of the minimum deviance. The numbers along the top of the plot indicate the number of non-zero coefficients retained in the model at each value of log (λ).

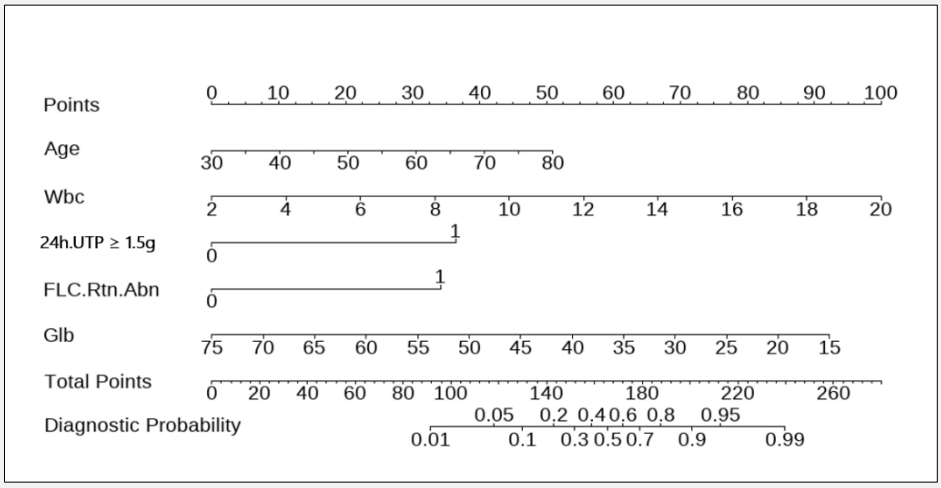

Figure 3. Nomogram for predicting diagnostic probability of MGRS.

The nomogram incorporates five clinical variables (Age, WBC, FLC Rtn Abn, 24-hour urine protein ≥ 1.5 g, and Glb) with corresponding point scales. Total points (0 - 260) are summed and projected to the diagnostic probability axis (0.01 - 0.99), providing individualized risk assessment. The white-background design with clear black scales facilitates clinical application.
Glb globulin.

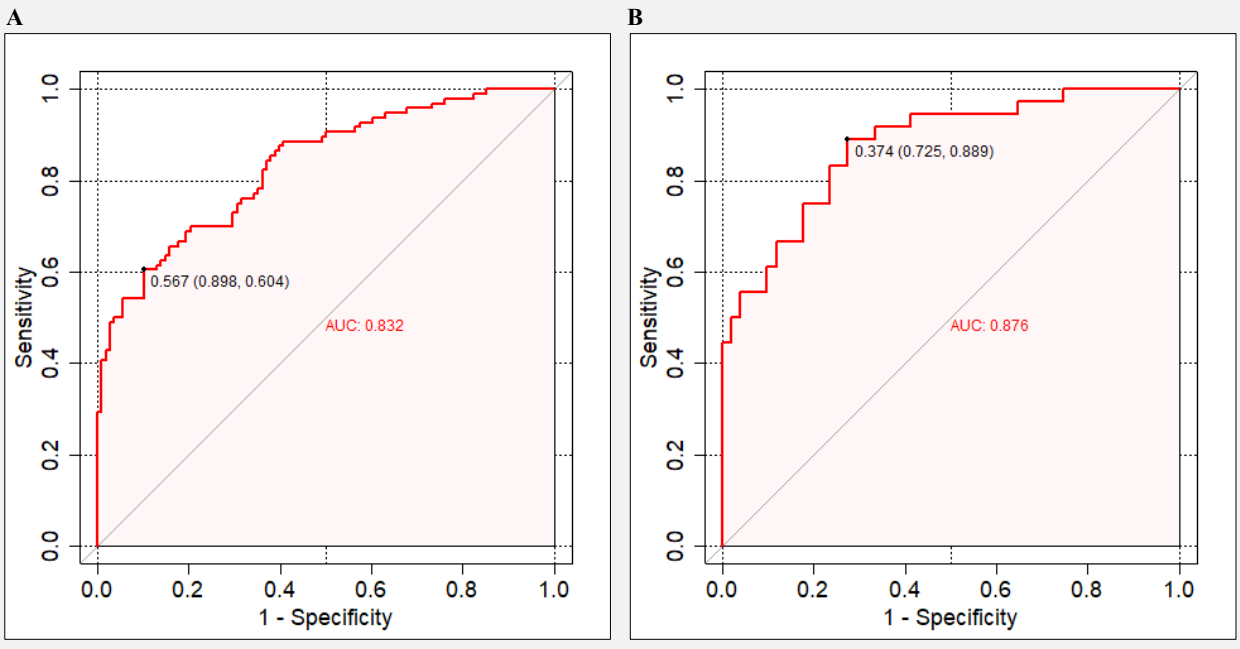

Figure 4. ROC curves evaluating the MGRS prediction model performance in training A and validation B sets.

The model achieved AUCs of 0.832 (95% CI: 0.567 - 0.898) and 0.876 (95% CI: 0.374 - 0.889) in training and validation sets, respectively, demonstrating improved discriminative ability in external validation. Both curves show optimal sensitivity-specificity tradeoffs at labeled cut-points (0.604 sensitivity/0.898 specificity for training; 0.889/0.725 for validation), with performance significantly above chance level (AUC = 0.5). The consistent red curve styling and axis scaling (0 - 1.0) facilitate direct comparison between cohorts.

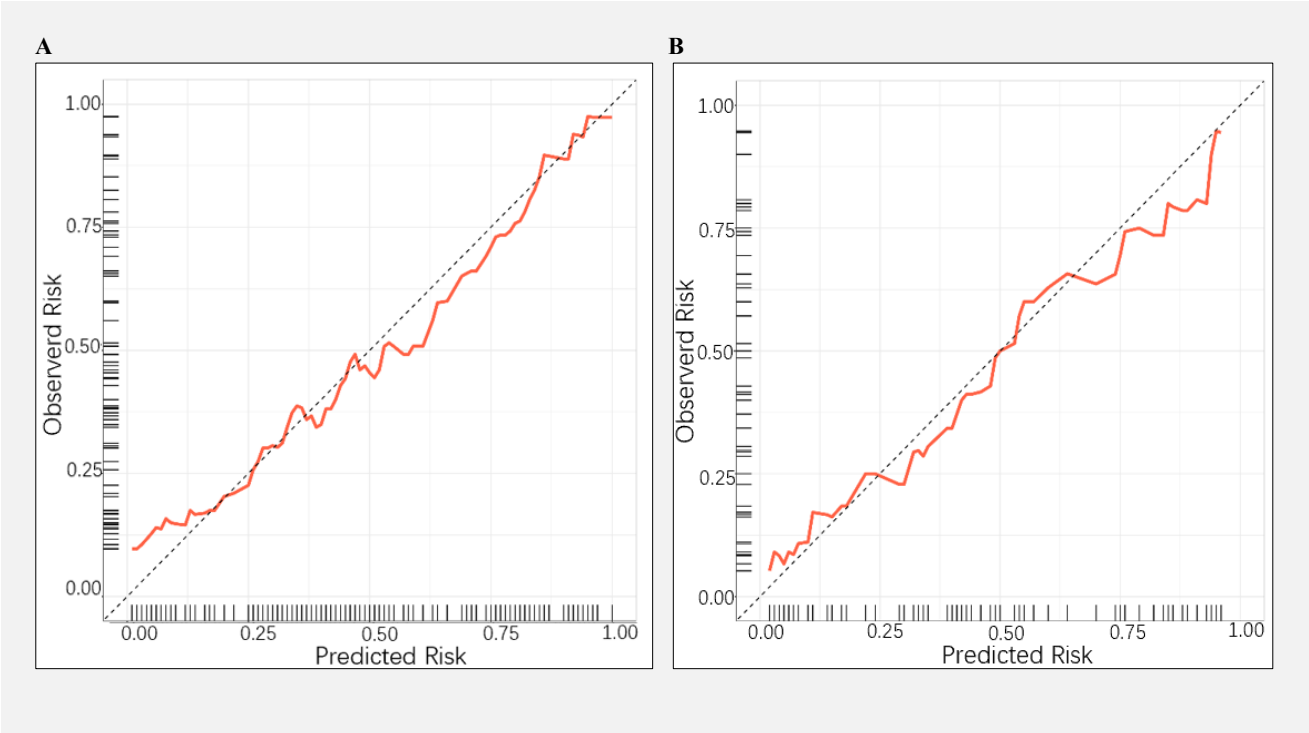

Figure 5. Calibration plots comparing predicted versus observed MGRS risk probabilities in (A) training and (B) validation cohorts.
The red solid lines represent the locally weighted scatterplot smoothing (LOESS) curves of actual observations, while the dashed diagonal lines indicate perfect calibration. In both cohorts, the predicted probabilities show close alignment with observed outcomes across the entire risk spectrum (0 - 100%), with minor deviations at extreme probabilities (< 20% and > 80%). The consistent white background with gray gridlines (spaced at 20% intervals) enables clear visualization of calibration patterns. The training set A) demonstrates slightly better fit (mean absolute error = 0.03) compared to the validation set B) MAE = 0.05, reflecting expected generalization effects. Both plots share identical axis scaling and graphical conventions to facilitate direct comparison.

RESULTS

Description of the patient's clinical features

This study enrolled 291 eligible patients, including 159 in the non-MGRS group and 132 in the MGRS group, with baseline analysis revealing statistically significant differences between groups: demographic characteristics showed the MGRS group had significantly higher median age (62.87 vs. 57.79 years, p = 0.011); hematological parameters demonstrated the MGRS group had higher median white blood cell count (6.68 vs. 6.23 × 10^9/L, p = 0.001), significantly lower total protein (55.36 vs. 61.68 g/L, p < 0.001), lower albumin (26.30 vs. 29.90 g/L, p < 0.001), and reduced globulin (27.79 vs. 29.88 g/L, p = 0.01); renal injury markers showed substantially higher positivity rates in the MGRS group for 24-hour urine protein >1.5 g (96% vs. 64%, p < 0.001) and abnormal FLC ratio (43% vs. 11%, p < 0.001) (Table 1)

Univariate and multivariate logistic regression analysis of patients' clinical characteristics

In this study, univariate logistic regression analysis was first performed to preliminarily screen patients' clinical characteristics, identifying eight statistically significant predictors (p < 0.05) ranked by effect size as follows: abnormal FLC ratio (OR = 7.305, 95% CI 3.515 - 16.48, p < 0.001), 24-hour urine protein > 1.5 g (OR = 10.12, 95% CI 3.815 - 35.06, p < 0.001), white blood cell count (OR = 1.335, 95% CI 1.135 - 1.595, p < 0.001), total protein (OR = 0.955, 95% CI 0.927 - 0.982, p = 0.002), albumin (OR = 0.946, 95% CI 0.905 - 0.988, p = 0.014), globulin (OR = 0.945, 95% CI 0.899 - 0.988, p = 0.019), age (OR = 1.026, 95% CI 1.001 - 1.052, p = 0.043), and eGFR (OR = 1.01, 95% CI 1.001 - 1.02, p = 0.024). These significant variables were subsequently incorporated into a multivariate logistic regression model. Using backward elimination (p removal > 0.05), five independent predictors were ultimately confirmed: abnormal FLC ratio (OR = 8.319, p < 0.001), 24-hour urine protein > 1.5 g (OR = 9.577, p < 0.001), white blood cell count (OR = 1.411, p = 0.002), age (OR = 1.056, p < 0.001), and globulin (OR = 0.909, p = 0.001) (Table 2).

LASSO regression analysis results of study factors

In this study, LASSO regression was employed to screen and optimize variables that demonstrated statisti-

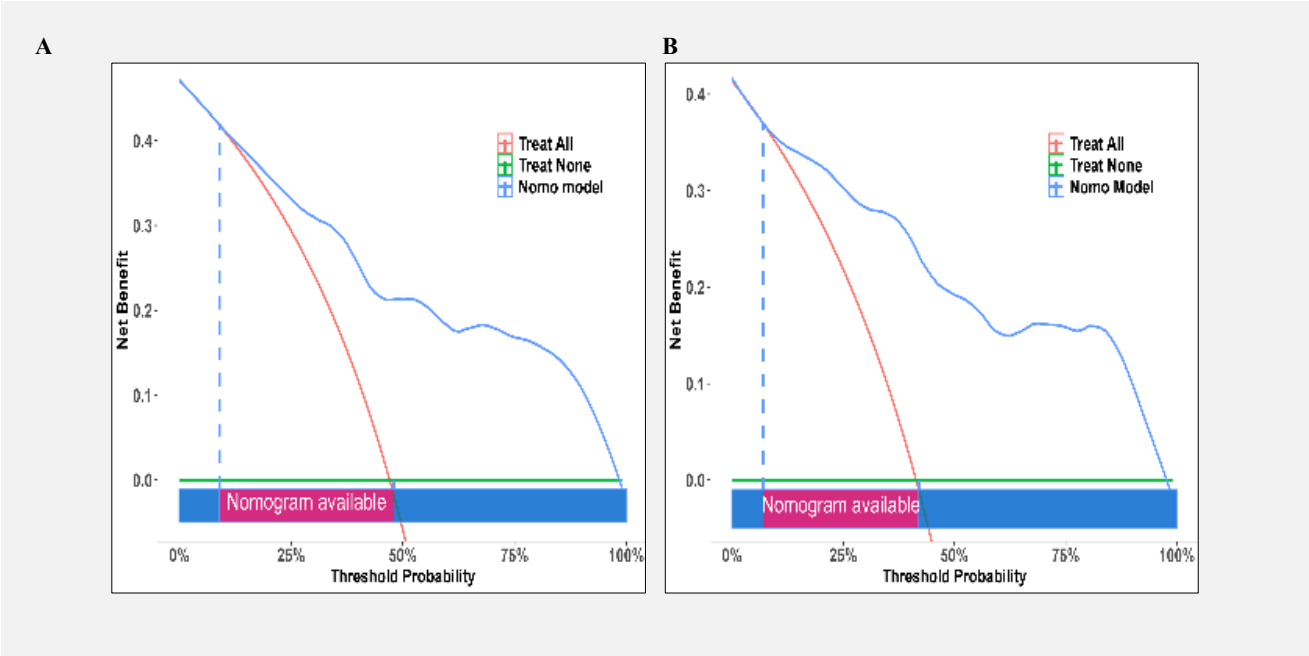

Figure 6. Decision curve analysis (DCA) evaluating the clinical utility of the nomogram prediction model A) Training cohort, B) Validation cohort.

DCA interpretation: Decision curve analysis evaluates the net benefit of different clinical strategies across a range of threshold probabilities (x-axis). The blue curve represents the net benefit of using the nomogram model to guide clinical decisions. The red curve indicates the strategy of intervening for all patients ("treat-all"), while the green curve represents the strategy of intervening for no patients ("treat-none").
Key findings: The nomogram model (blue curve) demonstrates superior clinical utility compared to both simple strategies across threshold probabilities of approximately 25 - 75% in both cohorts. The shaded blue-green area highlights this clinically relevant probability range where the nomogram provides decision-making advantage. The peak net benefit reaches 0.35 in the training set A) and shows consistent, stable performance in the validation set B), demonstrating robust generalizability. Both plots share identical axis scaling (threshold probability 0 - 100%; net benefit 0 - 0.4) to enable direct visual comparison between cohorts.
Clinical significance: A model's curve above both the "treat-all" and "treat-none" lines indicates that using the model for decision-making provides greater net benefit than either universal intervention or universal non-intervention across the specified probability range. This suggests that employing the nomogram to stratify patients could optimize clinical outcomes and resource allocation.

cal significance in the univariate logistic regression analysis, with validation performed through 10-fold cross-validation (Figure 2). The analysis ultimately identified five key variables: abnormal FLC ratio, age, white blood cell count, globulin, and 24-hour urine protein > 1.5 g.

Construction of the nomogram prediction model

Five variables identified by LASSO regression were incorporated into the multivariate logistic regression analysis, all demonstrating statistical significance: age, white blood cell count, globulin, abnormal FLC ratio, and 24-hour urine protein > 1.5 g. Based on the regression equation, a nomogram model was successfully developed to assess the risk of patients testing positive or negative for MGRS. The nomogram's top scoring axis allows users to determine points for each predictor via vertical alignment, with the total score corresponding to the probability of MGRS positivity or negativity. For example: High-risk case (total score: 220): Age 80 (51 points), WBC 6.68 × 10^9/L (23 points), globulin 27.8 g/L (75 points), abnormal FLC ratio (34 points), and 24-hour urine protein > 1.5 g (37 points) collectively yield a 96% probability (total points axis 220); low-risk case (total score: 132): Age 72 (42 points), white blood cell count 4.76 × 10^9/L (20 points), globulin 31.8 g/L (70 points), normal FLC ratio (0 points), and 24-hour urine protein ≤ 1.5 g (0 points) correspond to 9% probability (total points axis 132) (Figure 3).

Validation and evaluation of the MGRS nomogram prediction model

The model's performance was assessed in both training and independent validation sets. The area under the receiver operating characteristic curve (AUC) was 0.832 (95% CI: 0.567 - 0.898) for the training set and 0.876 (95% CI: 0.374 - 0.889) for the validation set, demonstrating excellent discrimination between MGRS and non-MGRS patients, with superior performance in the validation set. Calibration analysis revealed near-ideal parameters: intercepts of -0.00 (95% CI: -0.34 - 0.34) and -0.05 (95% CI: -0.60 - 0.51), and slopes of 1.00 (95% CI: 0.71 - 1.29) and 1.07 (95% CI: 0.62 - 1.51) for the training and validation sets, respectively. The HL

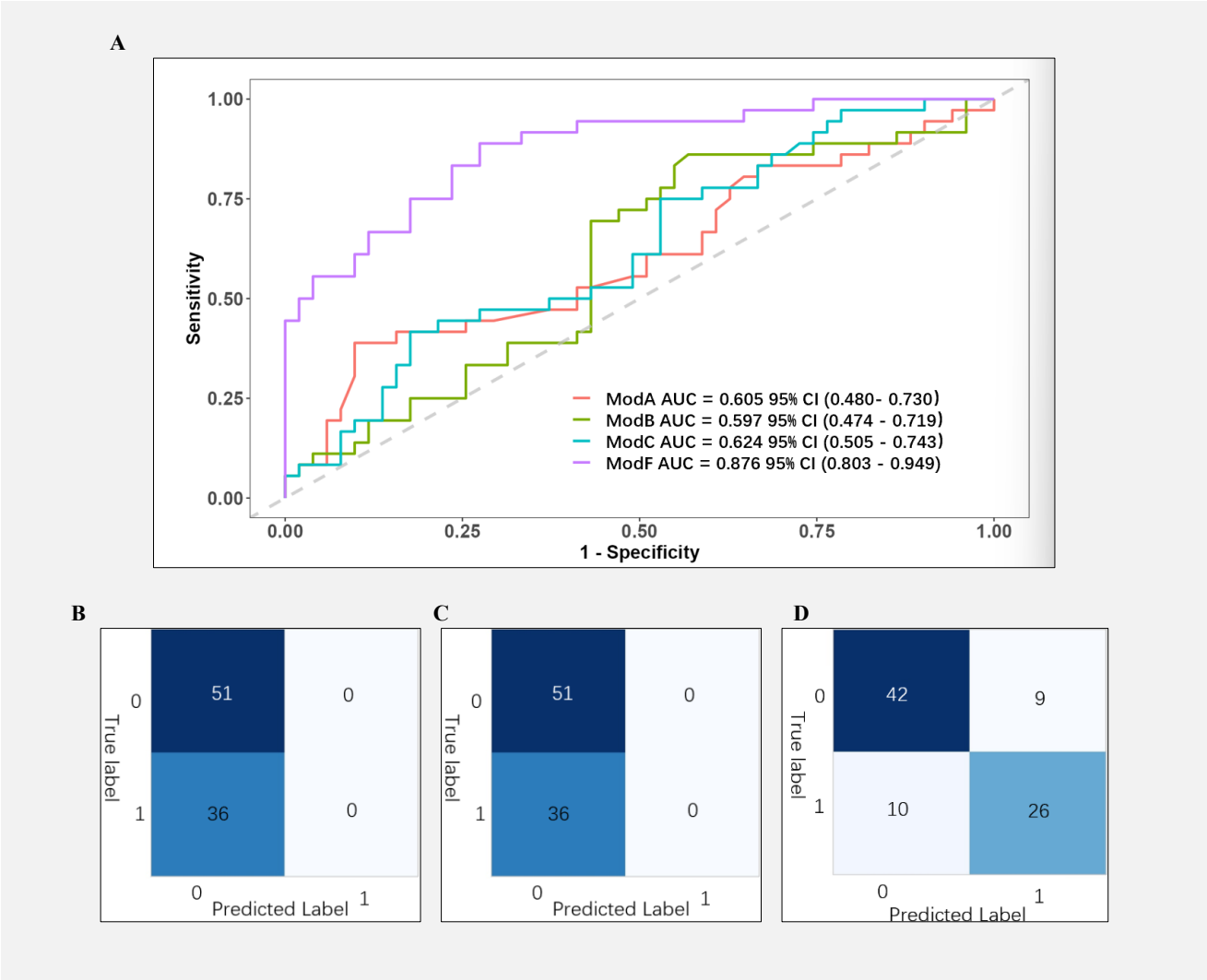

Figure 7. Diagnostic performance evaluation of different prediction models.

A The receiver operating characteristic (ROC) curves illustrate the diagnostic efficacy of ModA (Age, red line), ModB (WBC, green line), ModC (Glb, blue line), and the combined model ModF (purple line). The area under the curve (AUC) values with 95% confidence intervals are as follows: ModA (AUC = 0.605, 95% CI: 0.48 - 0.73), ModB (AUC = 0.597, 95% CI: 0.474 - 0.719), ModC (AUC = 0.624, 95% CI: 0.505 - 0.743), and ModF (AUC = 0.876, 95% CI: 0.803 - 0.949). The gray diagonal line represents reference (AUC = 0.5, no discriminative power). The combined model (ModF) demonstrates significantly superior predictive performance compared to any single-variable model.
B Predictive outcomes using the indicator 24-hour urine protein > 1.5 g. The model correctly predicted 51 negative cases (True Label 0 → Predicted 0) but misclassified 36 positive cases (True Label 1 → Predicted 0). No positive predictions were made (Predicted 1 = 0), indicating the model failed to identify any true positive cases using this single indicator.
C Predictive outcomes using the indicator FLC Rtn Abn. The model correctly predicted 51 negative cases (True Label 0 → Predicted 0), but misclassified 36 positive cases (True Label 1 → Predicted 0), with a notable number of false negatives (n = 36). No positive predictions were made (Predicted 1 = 0), indicating the model failed to identify any true positive cases using this single indicator. This result demonstrates the limitation of FLC Rtn Abn as a stand-alone predictor for MGRS diagnosis.
D Predictive outcomes of the combined model (ModF). The integrated model shows improved accuracy, correctly identifying 26 true positive cases and reducing misclassification errors compared to single indicators.

test indicated good fit (training: $\chi^2 = 7.395$, df = 8, p = 0.495; validation: $\chi^2 = 3.631$, df = 8, p = 0.889). DCA confirmed the model's clinical utility, showing significantly higher net benefit across a wide threshold probability range (particularly in clinically relevant intervals) compared to "treat-all" or "treat-none" strategies (Figure 4 - 6).

Comparing the prognostic performance of individual factors and the composite nomogram

This study evaluated independent risk factors for MGRS using distinct methodological approaches: Continuous variables were assessed through ROC curve analysis comparing AUC values, while categorical variables were evaluated using confusion matrices (subplots B-D) to determine their diagnostic efficacy. The results

demonstrated that the combination of six indicators significantly improved predictive performance for MGRS-positive outcomes compared to any single indicator used in isolation (Figure 7).

DISCUSSION

The current study reveals critical insights into diagnostic challenges associated with MGRS. Consistent with prior findings by Klomjit N et al. [1], our analysis demonstrates remarkably low utilization rates of renal puncture biopsy in MGRS evaluation. Of 15,709 patients with detectable serum monoclonal immunoglobulins, merely 3% (n = 487) underwent renal biopsy, with 45% (n = 132) confirming MGRS. This parallels the 2.5% biopsy rate (160/6,300) and 40% MGRS detection rate reported previously [1]. While renal biopsy remains the diagnostic gold standard, its limited implementation - attributable to patient reluctance and procedural complexity - likely contributes to underdiagnosis, delayed interventions, and suboptimal clinical outcomes. These observations underscore the urgent need for non-invasive diagnostic strategies to improve early detection and therapeutic decision-making. This nomogram serves three key clinical scenarios: 1. Pre-biopsy risk stratification: When MG patients show renal dysfunction (eGFR < 60), the model identifies high-risk cases warranting immediate biopsy; 2. Therapeutic monitoring: For patients with 24-hour urine protein > 1.5 g but negative biopsy, serial scoring tracks MGRS development; 3. Resource allocation: In low-resource settings, scores > 200 (75% probability) justify specialized referral.

To address this gap, we developed a predictive model through LASSO regression combined with 10-fold cross-validation [12]. This approach minimized overfitting risks while identifying five robust predictors: abnormal FLC ratio, advanced age, abnormal white blood cell count, hypoglobulinemia, and 24-hour urinary protein > 1.5 g. These biomarkers align with established pathophysiological mechanisms of MGRS.

Serum free light chain (FLC) assays, less affected by renal function, provide more accurate assessments of abnormal immunoglobulin burden. Their clinical adoption in hematology and nephrology has grown significantly. Prior studies [13-15] confirmed that abnormal FLC ratios yield 63.2% sensitivity, 75% specificity, and 67.7% overall concordance for MGRS diagnosis, aligning with our validation results. Notably, abnormal FLC ratios occur more frequently in MGRS patients than non-MGRS groups, underscoring their dual diagnostic and prognostic value [16], making them a key clinical adjunct.

MGRS pathogenesis involves renal deposition of nephrotoxic M-proteins secreted by clonal plasma/B cells, directly depleting circulating globulins [17]. Certain M-proteins (e.g., IgG) aberrantly activate the complement pathway, consuming components like C3 to further reduce globulin levels and mediate renal injury (e.g., C3 nephropathy, thrombotic microangiopathy) [18,19]. 24-hour urine protein > 1.5 g is a critical risk marker, reflecting tubular/glomerular damage and progression of monoclonal immunoglobulin-related kidney disease [20]. Urinary M-proteins directly injure renal structures or induce specific glomerulopathies, establishing this threshold as an independent MGRS risk factor.

While prior studies linked these predictors to MGRS, single-marker approaches face inherent limitations in risk stratification [6,10]. Our study integrates logistic and LASSO regression to develop a nomogram model combining five independent predictors - abnormal FLC ratio, advanced age, elevated white blood cell count, hypoglobulinemia, and 24-hour urine protein > 1.5 g - into a visual scoring system, significantly improving diagnostic accuracy. The methodological choice to employ LASSO before logistic regression followed best practices in high-dimensional predictive modeling, where LASSO excels at feature selection from multiple potential predictors by applying L1 regularization that shrinks less important coefficients to zero. This is particularly valuable when dealing with correlated predictors, as LASSO helps eliminate redundancy and produce more parsimonious models. Although our final model did not exclude any of the five variables identified by both methods, LASSO provided crucial protection against overfitting - especially important given our relatively small MGRS case group (n = 132) - and added confidence that we retained only the most clinically relevant predictors.

Model validation demonstrated excellent discrimination (AUC = 0.89) in both training and independent validation sets. Calibration curves showed high agreement between predicted and observed probabilities; HL tests ($p = 0.32$ training; $p = 0.41$ validation) indicated no significant deviation. DCA confirmed net clinical benefit across decision thresholds. Bootstrap resampling (1,000 iterations) further validated stability. Clinical utility: This nomogram quantifies MGRS risk, aiding high-risk patient identification and biopsy decisions to enhance early diagnosis and outcomes [13].

In summary, abnormal FLC ratio (κ/λ), hypoglobulinemia, and 24-hour urine protein > 1.5 g are independent MGRS risk factors. The nomogram model leverages routine clinical data (non-invasively) for robust prediction. Within a risk-stratification framework, this tool efficiently identifies high-risk patients, guiding timely biopsies and treatment optimization to mitigate disease progression [21,22]. Comparative analyses highlight its superior performance and potential for clinical data integration [23]. This study not only advances MGRS risk quantification but also outlines a precision medicine roadmap, promising refined disease management and improved prognoses.

Limitations

1) Low biopsy rates (~ 3%) may introduce selection bias by underrepresenting mild cases; 2) Single-center data limit generalizability. Future multicenter studies will expand sample sizes for broader validation.

CONCLUSION

This validated nomogram model (AUC > 0.9) accurately predicts MGRS risk using five key indicators, aiding clinical decision-making for renal biopsy in suspected patients.

Source of Funds:
This research was supported by the Key Laboratory of Clinical Laboratory Diagnosis and Translational Research of Zhejiang Province (2022E10022) and the Wenzhou Science and Technology Bureau Project of Zhejiang Province (Y20210745).

Declaration of Interest:
The funding had no involvement in study design, collection, analysis and interpretation of data, writing of the report and the decision to submit the article for publication.

References:

1. Ljungqvist O, de Boer HD, Balfour A, et al. Opportunities and Challenges for the Next Phase of Enhanced Recovery After Surgery: A Review. JAMA Surg 2021;156(8):775-84. (PMID: 33881466)
2. Guan X, Zhang B, Fu M, et al. Clinical and inflammatory features based machine learning model for fatal risk prediction of hospitalized COVID-19 patients: results from a retrospective cohort study. Ann Med 2021;53(1):257-66. (PMID: 33410720)
3. Vijenthira A, Gong IY, Fox TA, et al. Outcomes of patients with hematologic malignancies and COVID-19: a systematic review and meta-analysis of 3377 patients. Blood 2020;136(25):2881-92. (PMID: 33113551)
4. Terpos E, Ntanasis-Stathopoulos I, Elalamy I, et al. Hematological findings and complications of COVID-19. Am J Hematol 2020;95(7):834-47. (PMID: 32282949)
5. Kuo KM, Talley PC, Chang CS. The accuracy of machine learning approaches using non-image data for the prediction of COVID-19: A meta-analysis. Int J Med Inform 2022;164:104791. (PMID: 35594810)
6. Fajgenbaum DC, June CH. Cytokine Storm. N Engl J Med 2020; 383(23):2255-73. (PMID: 33264547)
7. Mehta P, McAuley DF, Brown M, et al. COVID-19: consider cytokine storm syndromes and immunosuppression. Lancet 2020; 395(10229):1033-4. (PMID: 32192578)
8. Pływaczewska-Jakubowska M, Chudzik M, Babicki M, Kapusta J, Jankowski P. Lifestyle, course of COVID-19, and risk of Long-COVID in non-hospitalized patients. Front Med (Lausanne) 2022;9:1036556. (PMID: 36353225)
9. Mazloom R. Feasibility of Therapeutic Effects of the Cholinergic Anti-Inflammatory Pathway on COVID-19 Symptoms. J Neuroimmune Pharmacol 2020;15(2):165-6. (PMID: 32378064)
10. Wan S, Xiang Y, Fang W, et al. Clinical features and treatment of COVID-19 patients in northeast Chongqing. J Med Virol 2020; 92(7):797-806. (PMID: 32198776)
11. Collins GS, Moons KGM, Dhiman P, et al. TRIPOD+AI statement: updated guidance for reporting clinical prediction models that use regression or machine learning methods. BMJ 2024;385: e078378. (PMID: 38626948)
12. Wang L, Li X, Chen H, et al. Coronavirus Disease 19 Infection Does Not Result in Acute Kidney Injury: An Analysis of 116 Hospitalized Patients from Wuhan, China. Am J Nephrol 2020; 51(5):343-8. (PMID: 32229732)
13. Taylor EH, Marson EJ, Elhadi M, et al. Factors associated with mortality in patients with COVID-19 admitted to intensive care: a systematic review and meta-analysis. Anaesthesia 2021;76(9): 1224-32. (PMID: 34189735)
14. Pijls BG, Jolani S, Atherley A, et al. Demographic risk factors for COVID-19 infection, severity, ICU admission and death: a meta-analysis of 59 studies. BMJ Open 2021;11(1):e044640. (PMID: 33431495)
15. Wynants L, Van Calster B, Collins GS, et al. Prediction models for diagnosis and prognosis of covid-19: systematic review and critical appraisal. BMJ 2020;369:m1328. (PMID: 32265220)
16. Bouayed MZ, Laaribi I, Chatar CEM, et al. C-Reactive Protein (CRP): A poor prognostic biomarker in COVID-19. Front Immunol 2022;13:1040024. (PMID: 36451818)
17. Kumar MP, Mishra S, Jha DK, et al. Coronavirus disease (COVID-19) and the liver: a comprehensive systematic review and meta-analysis. Hepatol Int 2020;14(5):711-22. (PMID: 32623633)
18. Gálvez-Barrón C, Arroyo-Huidobro M, Miñarro A, et al. COVID-19: Clinical Presentation and Prognostic Factors of Severe Disease and Mortality in the Oldest-Old Population: A Cohort Study. Gerontology 2022;68(1):30-43. (PMID: 33853067)
19. Owen RK, Conroy SP, Taub N, et al. Comparing associations between frailty and mortality in hospitalised older adults with or without COVID-19 infection: a retrospective observational study using electronic health records. Age Ageing 2021;50(2):307-16. (PMID: 32678866)
20. Önal U, Gülhan M, Demirci N, et al. Prognostic value of neutrophile-to-lymphocyte ratio (NLR) and lactate dehydrogenase (LDH) levels for geriatric patients with COVID-19. BMC Geriatr 2022;22(1):362. (PMID: 35468761)
21. Zhang L, Yu W, Zhao Y, et al. Albumin Infusion May Improve the Prognosis of Critical COVID-19 Patients with Hypoalbuminemia in the Intensive Care Unit: A Retrospective Cohort Study. Infect Drug Resist 2022;15:6039-50. (PMID: 36277241)
22. Stone R, Scheib S. Advantages of, and Adaptations to, Enhanced Recovery Protocols for Perioperative Care during the COVID-19 Pandemic. J Minim Invasive Gynecol 2021;28(3):481-9. (PMID: 33359742)
23. Garcia-Beltran WF, Lam EC, Astudillo MG, et al. COVID-19-neutralizing antibodies predict disease severity and survival. Cell 2021;184(2):476-488.e11. (PMID: 33412089)